

## Fluid-Structure Interaction of a Cylinder Rolling Down an Incline under Gravity

F. Y. Houdroge<sup>1</sup>, K. Hourigan<sup>1,2</sup>, T. Leweke<sup>3</sup> and M. C. Thompson<sup>1</sup>

<sup>1</sup>Fluids Laboratory for Industrial and Aeronautical Research, FLAIR  
 Department of Mechanical and Aerospace Engineering  
 Monash University, VIC, 3800, Australia

<sup>2</sup>Division of Biological Engineering, Faculty of Engineering  
 Monash University, VIC, 3800, Australia

<sup>3</sup>Institut de Recherche sur les Phénomènes Hors Equilibre, IRPHE  
 CNRS/Universités Aix-Marseille,  
 49, rue Frédéric Joliot-Curie, B.P. 146, F-13384 Marseille Cedex 13, France

### Abstract

The flow characteristics and fluid forces experienced by a body rolling down an inclined plane under gravity are examined through numerical modelling. This problem has been studied for a wide range of Reynolds numbers, inclination angles and density ratios. Two cases are considered: the first is a reference case of a cylinder rolling on a horizontal wall at a constant velocity, and the second consists of the cylinder rolling down an incline with a velocity that varies with the time-varying forces it experiences. The time-dependent motion of the body and the flow field, and their relationship to the drag, lift and torque were analysed to better understand of the governing physical mechanisms, and the relationship to the constant speed case.

### Introduction

We investigate the problem of a viscous incompressible flow past a circular cylinder rolling along a solid surface. This problem has relevance to a number of important physical applications, including biological flows such as cell-wall interactions, and two-phase flows for which particle interactions near boundaries are not well-understood.

Studies by Taneda [8] showed that positioning a stationary cylinder close to a wall acts to stabilize the wake. Indeed, proximity to a wall is able to alter the flow through the suppression of vortex shedding when the wall distance is less than a critical value [3]. For gaps greater than this critical value, the flow approaches that past a cylinder in free stream. Nishino et al. [4], suggested that the nearby wall can have an effect similar to placing a splitter plate in the wake. They proposed that the wall limits the growth of disturbances that result in an absolute instability and the onset of the characteristic Bénard-von Kármán shedding. Rather than through an absolute instability, they observed that the wake is better characterised as convectively unstable as the cylinder approaches a wall.

Recent work by Stewart et al. [6, 7] examined the wakes of circular cylinders and spheres rolling along a wall at a constant speed, showing a multitude of different wake states exist as the Reynolds number was increased. The wall, of course, changes the nature of the wake relative to the situation when the body is placed in free stream. In particular, as discussed above, the absolute instability responsible for Bénard-von Kármán shedding is suppressed, and the natural wake centreline symmetry is removed, leading to quite different flow dynamics and transitions.

For the work reported in this paper, the body (a cylinder) rolls along the wall under the influence of gravity. At low Reynolds number, a steady wake develops, so that the final state is the body rolling along at a constant terminal velocity. As the

Reynolds number (or inclination angle) is increased, however, the wake eventually becomes unsteady. For bodies close to neutral buoyancy, the fluctuating forces associated with the unsteady wake mean that the final kinematic state is not a constant terminal velocity. This study examines this flow problem in more detail.

### Description of the Problem and Methodology

Consider a cylinder moving in the intuitive sense of forward rolling ( $\alpha = \omega R/U = 1$ , where  $\omega$  is the angular velocity,  $U$  is the centre of mass speed and  $R$  is the cylinder radius, as defined by [7]) along a plane wall through a quiescent fluid. The problem setup is shown in figure 1.

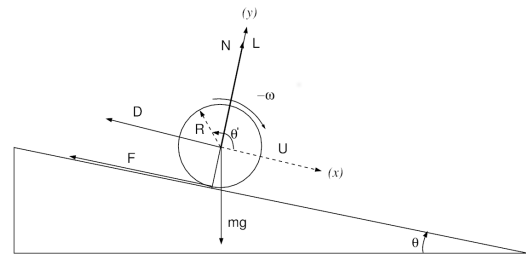


Figure 1: Problem setup and parameter definition. This also shows the forces acting and the alignment of the axes. See text for details.

In terms of computational modelling, in order to simplify the analysis, the frame of reference is attached to the centre of the cylinder: this is equivalent to the fluid and wall moving past the fixed body. The motion of the cylinder - and thus the velocity of the fluid and the wall - may be fixed at a constant value or free to vary with the different problem parameters.

As part of this study, two cases were considered: the first is the reference case of a cylinder, submerged in a fluid, rolling at a fixed velocity (referred to as the “fixed rolling case”) along a horizontal wall, and the second is that of a cylinder rolling along an inclined wall under gravity with no restrictions on the body’s velocity (referred to as the “free rolling case”). For both sets of simulations, wide ranges of values were considered for the Reynolds number, the gravity ( $g$ ) or inclination angle of the wall ( $\alpha$ ), through the parameter  $g \sin \alpha$  - and thus the velocity of the fluid and the wall - may be fixed at a constant value or free to vary with the different problem parameters. These parameters can be combined into two governing non-dimensional parameters: a generalised Reynolds number,  $Re_f$ , and the density ratio,  $\beta$ , as discussed below. This investigation brings a further understanding of the importance of each parameter and its influence on the

behaviour of the fluid and the cylinder.

The model requires a coupling between the equations that describe, on the one hand, the motion of the fluid and on the other hand, the motion of the cylinder. The rotation of the cylinder changes the velocities on the boundary which in return induces flow in the fluid, and the fluid influences the angular velocity of the cylinder by exerting forces and torques upon it. The governing equations are the law of motion for the cylinder, the viscous incompressible Navier–Stokes equations and the continuity equation for the fluid flow (equations (1), (2) and (3) below). The relation between the movement of the cylinder and the flow of the surrounding fluid is therefore established through the velocity of the cylinder as follows:

$$\frac{du_c}{dt} = \frac{2}{3} \left[ \left(1 - \frac{1}{\beta}\right) g \sin \alpha - \frac{D}{\pi R^2 \rho_c} - \frac{T}{\pi R^3 \rho_c} \right], \quad (1)$$

$$\nabla \cdot \mathbf{u}_f = 0 \quad (2)$$

$$\frac{\partial \mathbf{u}_f}{\partial t} + \mathbf{u}_f \cdot \nabla \mathbf{u}_f = -\frac{1}{\rho_f} \nabla P + \nu \nabla^2 \mathbf{u}_f - \frac{d\mathbf{u}_c}{dt}, \quad (3)$$

where  $\mathbf{u}_f(x, y, z, t) = (u, v, w)$  and  $\mathbf{u}_c(x, y, z, t) = (u_c, 0, 0)$  are the velocities of the fluid and the cylinder respectively,  $\rho_f, \rho_c$  their densities,  $\alpha$  the slope of the wall,  $g$  the gravitational acceleration,  $D$  the drag force per unit span (pressure plus viscous components) and  $T$  the viscous torque per unit span.

### Non-Dimensionalisation of the Equations

The physical variables were non-dimensionalised as follows. The length scale is provided by cylinder radius  $R$  which can be combined with combinations of the other controlling parameters ( $g, \alpha, \rho_c$  and  $\rho_f$ ) to define velocity and time scalings:

$$V_f = \left( \frac{\Delta p}{\rho_f} R g \sin \alpha \right)^{\frac{1}{2}} \text{ and } \tau = \left( \frac{R}{\frac{\Delta p}{\rho_f} g \sin \alpha} \right)^{\frac{1}{2}}, \text{ respectively. The}$$

pressure is then scaled by  $\rho_f V_f^2$  where  $\Delta p = \rho_c - \rho_f$ .

With these definitions, the non-dimensional form of the Navier–Stokes equation (3) is:

$$\frac{\partial \mathbf{u}_f^*}{\partial t^*} + \mathbf{u}_f^* \cdot \nabla^* \mathbf{u}_f^* = -\nabla^* P^* + \frac{1}{Re_f} \nabla^{*2} \mathbf{u}_f^* - \frac{d\mathbf{u}_c^*}{dt^*}, \quad (4)$$

where the Reynolds number is defined as  $Re_f = \frac{RV_f}{\nu}$ . The acceleration equation (1) takes on the following form:

$$\frac{du_c^*}{dt^*} = \frac{2}{3\beta} \left( 1 - \frac{C_D}{\pi} - \frac{C_T}{\pi} \right), \quad (5)$$

where  $\beta = \frac{\rho_c}{\rho_f}$  is the ratio of the body density to the density of the fluid,  $C_D$  and  $C_T$  are the drag force and torque coefficients.

For the fixed rolling case, the speed ( $U$ ) of the body is prescribed and the Navier–Stokes scaling is standard with the Reynolds number defined using the fixed velocity of the body,  $Re_c = U(2R)/\nu$ . For convenience it is useful to sometimes use this Reynolds number for the freely rolling case also, in which case the velocity scale is then taken as the mean terminal velocity of the cylinder.

### Numerical Scheme

The code used for this analysis has previously been tested and used with flows around cylinders [10, 5] and spheres [9, 11] (amongst others). The equations are discretised using a semi-implicit spectral-element scheme with iterative time-stepping.

A fractional-step method [1] is used for the temporal discretisation. The approach adopted is given in [2]. For simplicity, the majority of the results are presented in the non-dimensional form.

## Results

### Fixed Rolling vs. Free Rolling

For convenience, for all simulations, the cylinder's radius is set to 0.5 and its velocity to 1 in the fixed rolling case. In order to initially compare the different body forces between the two cases, we chose a situation where the terminal velocities in the final state of the system were similar. An initial scanning through parameters revealed that for  $Re_c = 100$ , this condition is met when  $g \sin \alpha = 0.5$  and  $\beta = 7$  for the freely rolling case.

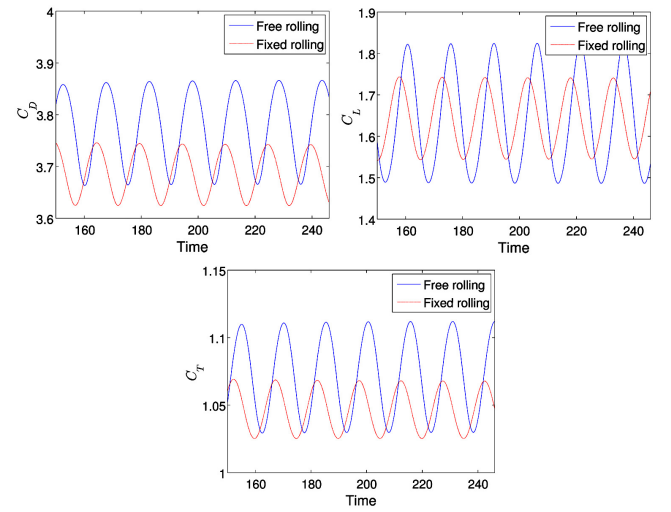


Figure 2: Plots comparison of the drag, lift and torque coefficients as a function of time for the two cases when the terminal velocity is similar. Free rolling case (blue line):  $Re_c = 100, U = 1$ . Fixed rolling case (red dash):  $Re_c = 100, U = 1$  which was equivalent to  $g \sin \alpha = 0.5$  and  $\beta = 7$ .

Figure 2 shows the behaviour of the drag, lift and torque coefficients as a function of time in both cases for  $Re_c = 100$  and a mean terminal velocity in the freely rolling case equal to 1. Each period corresponds to the shedding of a vortex. For each case, the body forces fluctuate around a similar value. Even though for the freely rolling case, the velocity varies throughout the shedding cycle, the shedding frequency is still relatively close to the fixed rolling case. What varies mostly is the amplitudes of the oscillations, which are significantly higher when the body is free to roll and spin in the fluid under the influences of the forces acting.

We found that the critical value of the Reynolds number for both cases at which the flow becomes unstable was approximately ( $Re_c = 90$ ). This is in good agreement with the one found by Stewart *et al.* [7]. Past this value, vortices start forming and shedding into the wake of the cylinder (as shown in figure 3).

A first look at both cases for varying Reynolds numbers helps us in comparing how the different fluid forces and torques behave when the cylinder is fixed and free to roll, as shown in figure 4. For the free rolling simulations (on the right),  $\beta$  and  $g \sin \alpha$  were fixed at 2.0 and 0.5 respectively.

For both simulations, the drag, lift and torque coefficients behave similarly: they all decrease as the Reynolds number increases. The variation in the mean drag force is insignificant for

Re = 60



Re = 100



Re = 150



Figure 3: Process of vortex formation and shedding in the wake of the cylinder as the Reynolds number increases.

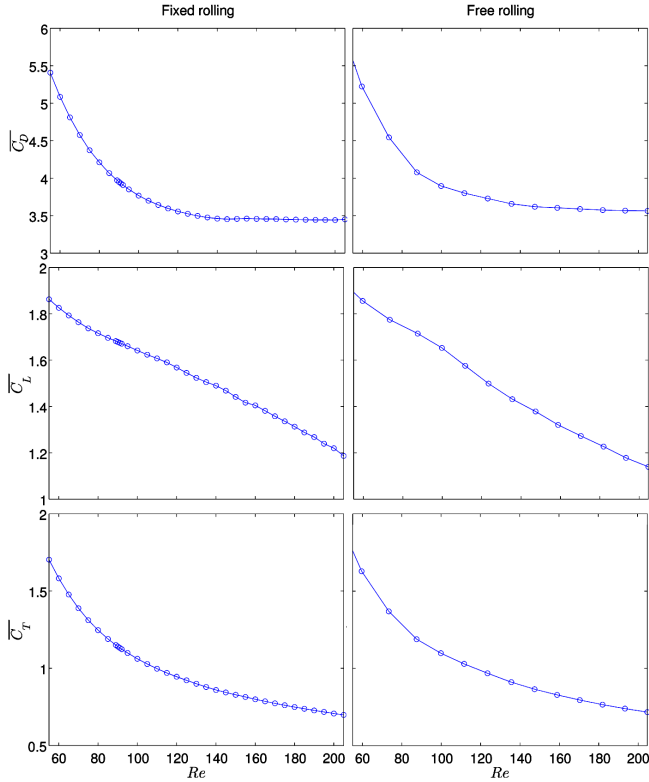


Figure 4: Graphs of the mean drag, lift and torque coefficients as a function of Reynolds number for the fixed (left) and the free (right) rolling cases. In the latter case,  $\beta = 2$  and  $g \sin \alpha = 0.5$ . The Reynolds number in this case is based on the mean terminal velocity found from post-processing the data.

$Re_c > 140$ , whereas the mean lift force decreases almost linearly with  $Re_c$ . These results are consistent with prior studies. For  $Re_c < 90$ , when the final flow is steady, there is an exact match between the cases, with some variation for the higher Reynolds number cases, as quantified below.

When the cylinder is free to roll, we extended this study for different values of density ratios and inclination angles and analysed the behaviour of the different forces, torques and velocities in order to understand how they influence the dynamics of the problem.

### Effects of the Inclination Angle of the Wall and the Density Ratio

The effect that the slope of the wall, which influences the gravitation force along the wall, and the ratio of densities have on the different body forces and torques was then examined. The viscosity coefficient was set to 0.01, while  $g \sin \alpha$  (with  $\beta = 2$  fixed) varies from 0.1 to 7 and  $\beta$  (with  $g \sin \alpha = 0.5$  fixed) from 1.5 to 11.5. The results are specified as a function of  $Re_f$ , which governs the asymptotic state of the system, as will be explored in the next section.

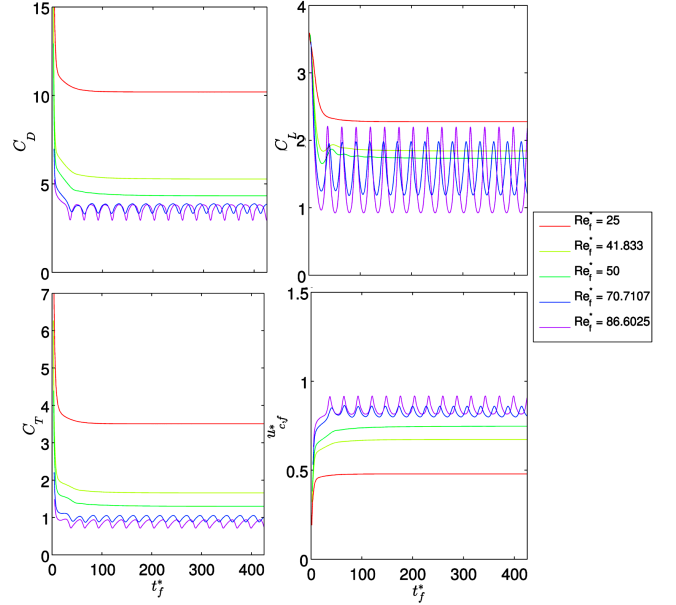


Figure 5: Temporal evolution of the drag force, the lift force, the viscous torque and the velocity as a function of  $t^*$  for  $25 \leq Re_f \leq 86.6$ .

The evolution of the drag force, the lift force, the viscous torque and the velocity as a function of  $t^*$  for different values of  $Re_f$  are shown in figure 5. The flow becomes unstable for  $Re_f \geq 56$ . For the highest Reynolds number cases, the oscillations in the drag and rolling speed vary by the order of 10% in the asymptotic state, whilst the lift coefficient varies by a factor of two.

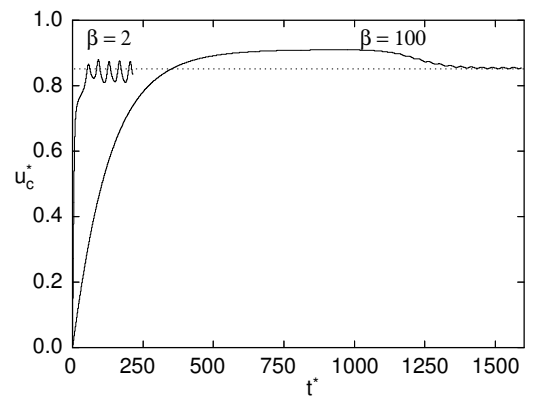


Figure 6: Evolution of the rolling speed for the same  $Re_f = 70.7$  demonstrating that it determines the final average flow state.  $\beta$  is given in the figure with  $g \sin \alpha$  adjusted to match  $Re_f$ . Both cases used  $\nu = 0.005$ .

### Asymptotic scaling

Figure 6 shows the rolling speed evolution for two cases with the same  $Re_f$  but widely differing density ratios. Whilst the initial evolution is distinctly different, the final mean asymptotic flow speed approaches the same value. This demonstrates that the chosen time and length scales allow the final state to be a function of the modified Reynolds number only. Of course, the size of the oscillations is dependent on the density ratio, since it is easier to change the velocity of a lighter cylinder. The oscillation period depends on the final velocity—so is the same (or very similar) for these cases.

### Lift Force

For the values of  $0.5 \leq g \sin \alpha \leq 7$  and  $1.1 \leq \beta \leq 12.5$  that were considered throughout this study, the value of the lift force never exceeded the normal gravitational force towards the wall ( $m^* g \cos \alpha$ ). Thus the body is always attracted towards the wall, at least within these ranges.

### Prediction of the Mean Terminal Velocity

The goal here is to calculate a mean terminal velocity of the free rolling cylinder using the fixed rolling simulations. To do so, let's consider the non-dimensional form of equation (5) with  $U_{f,free} \neq 1$ . In the asymptotic state, the mean value of the rate of change of the velocity approaches zero. Using equation (5) this gives

$$U_{f,free} = \left( \frac{\pi}{C_D + C_T} \right)^{\frac{1}{2}} \quad (6)$$

The drag and torque coefficients  $C_D$  and  $C_T$  are calculated using the drag force  $D$  and viscous torque  $T$  extracted from the fixed rolling simulations.

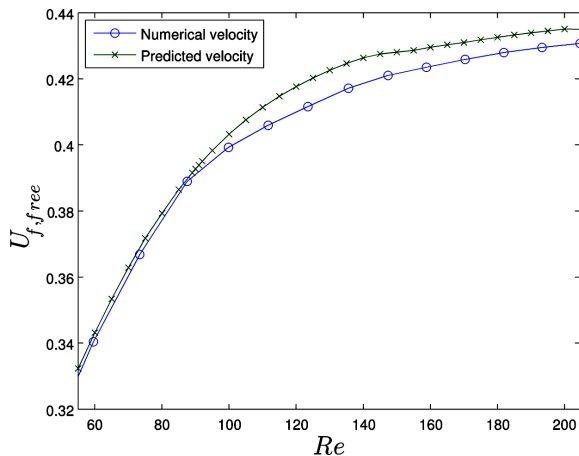


Figure 7: Comparison of the predicted mean terminal velocity variation to that obtained from freely rolling simulations.

Figure 7 shows the comparison of the predicted mean terminal velocity based on freely rolling results, together with direct predictions from freely rolling simulations for  $\beta = 2$ ,  $g \sin \alpha = 0.5$  and a varying Reynolds number. Essentially, and as expected, the two curves match prior to transition at  $Re_c > 90$  and deviate past this point. This divergence is due to the fact that the freely rolling cylinder does not achieve a steady final state.

### Conclusions

Following a study on the fluid-structure interaction of a cylinder rolling down an incline under different conditions, information was obtained on the parameters that govern the dynamics of

such systems. In the freely rolling case, the cylinder reaches a steady final speed for  $Re_c < 90$ , but above this value the fluid forces and hence the cylinder velocity oscillate about a mean state. These oscillation can be of order 10% for the drag and speed, and 100% for the lift. A scaling analysis indicates that the asymptotic behaviour, in terms of *mean* fluid forces and cylinder speed, depend only on a modified Reynolds number,  $Re_f$ . The oscillation amplitudes of the cylinder speed and force coefficients, however, still depend on the density ratio, since lighter bodies are more susceptible to the same fluid force. Of interest, force coefficients obtained from simulations of a fixed rolling cylinder can be used to approximate the mean final state of a freely rolling cylinder to reasonably good accuracy ( $\sim 1\%$ ).

### Acknowledgements

This research was supported by an Australian Research Council Discovery Project Grant DP130100822. We also acknowledge computing time support through National Computing Infrastructure projects D71 and N67.

### References

- [1] Chorin, A.J., Numerical solution of the Navier–Stokes equations, *Mathematics of Computation*, **22**, 1968, 745–762.
- [2] Karniadakis, G.E., Israeli, M. and Orszag, S.A., High-order splitting methods for the incompressible Navier–Stokes equations, *Journal of Computational Physics*, **97**, 1991, 414–443.
- [3] Lei, C., Cheng, L. and Kavanagh, K., Re-examination of the effect of a plane boundary on force and vortex shedding of a circular cylinder, *Journal of Wind Engineering and Industrial Aerodynamics*, **80**(30), 1999, 263–286.
- [4] Nishino, T., Roberts, G.T. and Zhang, X., Vortex shedding from a circular cylinder near a moving ground, *Physics of Fluids*, **19**, 2007, 12.
- [5] Ryan, K., Thompson, M.C. and Hourigan, K., Three-dimensional transition in the wake of bluff elongated cylinders, *Journal of Fluid Mechanics*, **538**, 2005, 1–29.
- [6] Stewart, B.E., Thompson, M.C., Leweke, T. and Hourigan, K., Numerical and experimental studies of the rolling sphere wake, *Journal of Fluid Mechanics*, **643**, 2010, 137–162.
- [7] Stewart, B.E., Thompson, M.C., Leweke, T. and Hourigan, K., The wake behind a cylinder rolling on a wall at varying rotation rates, *Journal of Fluid Mechanics*, **648**, 2010, 225–256.
- [8] Taneda, S., Visualization of Separating Stokes Flows, *Journal of the Physical Society of Japan* **46**, 1979, 1935.
- [9] Thompson, M.C., Leweke, T. and Provansal, M., Kinematics and dynamics of sphere wake transition, *Journal of Fluids and Structures*, **15**, 2001, 575–586.
- [10] Thompson, M.C., Leweke, T. and Williamson, C.H.K., The physical mechanism of transition in bluff body wakes, *Journal of Fluids and Structures*, **15**, 2001, 607–616.
- [11] Thompson, M.C., Hourigan, K., Cheung, A. and Leweke, T., Hydrodynamics of a particle impact on a wall, *Applied Mathematical Modelling*, **30**(11), 2006, 1356–1369.